

ChemComm

Accepted Manuscript



This article can be cited before page numbers have been issued, to do this please use: S. Feng, H. Xu, C. Zhang, Y. Chen, J. Zeng, D. Jiang and J. Jiang, *Chem. Commun.*, 2017, DOI: 10.1039/C7CC07024A.



This is an Accepted Manuscript, which has been through the Royal Society of Chemistry peer review process and has been accepted for publication.

Accepted Manuscripts are published online shortly after acceptance, before technical editing, formatting and proof reading. Using this free service, authors can make their results available to the community, in citable form, before we publish the edited article. We will replace this Accepted Manuscript with the edited and formatted Advance Article as soon as it is available.

You can find more information about Accepted Manuscripts in the [author guidelines](#).

Please note that technical editing may introduce minor changes to the text and/or graphics, which may alter content. The journal's standard [Terms & Conditions](#) and the ethical guidelines, outlined in our [author and reviewer resource centre](#), still apply. In no event shall the Royal Society of Chemistry be held responsible for any errors or omissions in this Accepted Manuscript or any consequences arising from the use of any information it contains.

Bicarbazole-based redox-active covalent organic frameworks for ultrahigh-performance energy storage[†]

 Shi Feng,^a Hong Xu,^b Chong Zhang,^a Yu Chen,^a Jinghui Zeng,^a Donglin Jiang^{*b} and Jia-Xing Jiang^{*a}

 Received 00th January 20xx,
Accepted 00th January 20xx

DOI: 10.1039/x0xx00000x

www.rsc.org/

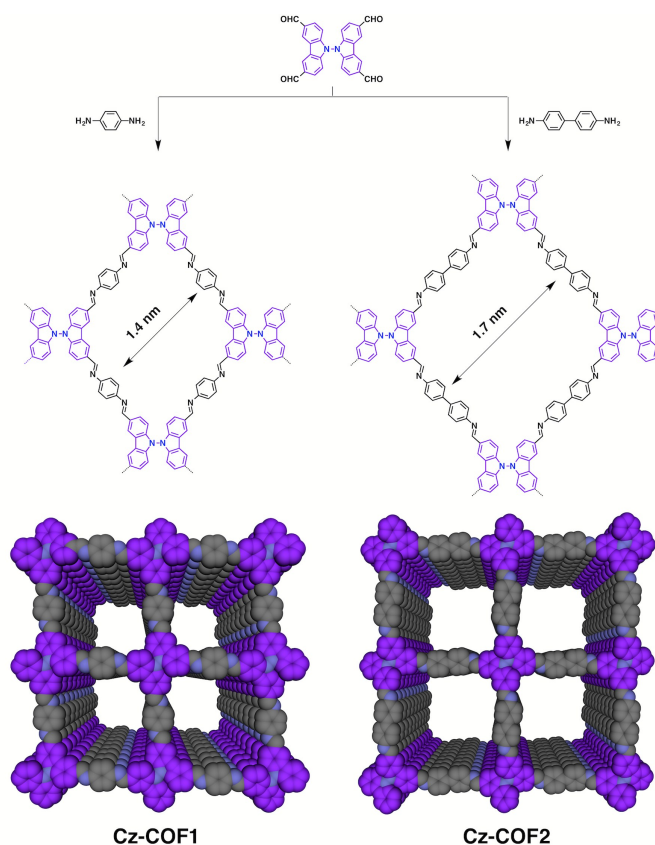
A highly redox-active building block, bicarbazole, is developed as a monomer for designing crystalline porous covalent organic frameworks and is successfully integrated to the vertices of microporous tetragonal frameworks, leading to densely aligned redox-active arrays. The frameworks with large porosity and high accessibility of the redox-active sites exhibit synergistic structural effects and achieve ultrahigh-performance energy storage.

Energy storage is a must for sustainable development.¹⁻⁵ Considering ever-increasing power consumption and efficient energy utilization, developing high-performance materials for energy storage is urgent and essential.

Covalent organic frameworks (COFs) are a class of crystalline porous polymer that integrates various π -units into periodically ordered π -arrays and creates porous structures.⁶⁻⁹ By virtue of their excellent stability, well-defined pores, and ordered skeletons, COFs have emerged as functional materials that are promising for gas adsorption,^{10,11} light emitter,^{12,13} semiconductor,^{14,15} proton conduction,^{16,17} catalysis,¹⁸⁻²⁰ environmental remediation,^{21,22} energy conversion and storage.²³⁻³⁰ Owing to the lack of suitable redox-active building blocks and the difficulty in the synthesis of crystalline skeletons, design and synthesis of redox-active COFs are still very limited and remain a chemical challenge.

In this study, we developed a typical redox-active π -unit, i.e., bicarbazole, as a monomer for the design and construction of crystalline porous COFs and successfully integrated the bicarbazole units into the vertices of microporous tetragonal

COFs (Scheme 1). These COFs feature large porosity of open one-dimensional (1D) channels and densely aligned π -arrays of redox-active bicarbazole sites. We highlight their synergistic effect on achieving ultrahigh-performance energy storage.



Scheme 1. Design and synthesis of redox-active bicarbazole (Cz)-based COFs (Cz-COFs). The bottom layer shows the stacking structures in which the Cz units (purple) occupy the vertices and yield dense arrays of the redox-active Cz sites and 1D open channels.

The newly designed microporous bicarbazole COFs (Scheme 1, Cz-COF1 and Cz-COF2) with dense redox-active units and 1D open micropores were designed using a [C₂ + C₂] topology diagram and successfully synthesized via a Schiff-base

^a Key Laboratory of Applied Surface and Colloid Chemistry (Shaanxi Normal University), Ministry of Education, Key Laboratory for Macromolecular Science of Shaanxi Province, School of Materials Science and Engineering, Shaanxi Normal University, Xi'an 710062, Shaanxi, P. R. China.
E-mail: jiaxing@snnu.edu.cn

^b Field of Energy and Environment, School of Materials Science, Japan Advanced Institute of Science and Technology, 1-1 Asahidai, Nomi 923-1292, Japan.
E-mail: djjiang@jaist.ac.jp

[†] Electronic Supplementary Information (ESI) available: Details for synthesis and characterizations, lithium ion batteries measurements, TGA traces, IR and solid state ¹³C-NMR spectra, SEM and TEM images, and additional simulations. See DOI: 10.1039/x0xx00000x

condensation reaction of tetraformyl-bicarbazole and aromatic diamines. The resulting Cz-COFs were insoluble in common organic solvents and were chemically stable in various aqueous conditions including HCl (1 M) and NaOH (1 M) for 3 days. The COFs were characterized by various analytic methods (Figs. S1-S18, ESI[†]). Elemental analysis revealed that the C, H, and N contents were close to the theoretical values of infinite 2D sheets (Table S1, Electronic Supporting Information, ESI[†]). Thermogravimetric analysis revealed that both Cz-COFs are stable up to 450 °C in nitrogen (Fig. S1, ESI[†]). The Fourier transform infrared spectra showed strong C=N stretching vibration bands at 1618 cm⁻¹ (Fig. S2, ESI[†]), indicating the formation of imine linkages.

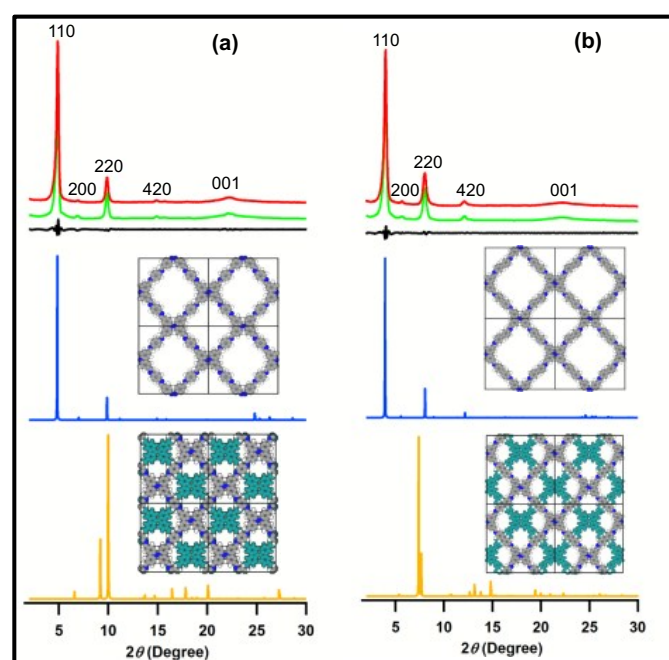


Fig. 1 PXRD profiles of (a) Cz-COF1 and (b) Cz-COF2 for experimentally observed (red), Pawley refined (green), difference between experimental and calculated data (black), calculated for the AA (blue) and AB (yellow) stacking models. Insets are structures for Cz-COF1 and Cz-COF2 with the AA (upper) and AB (bottom) stacking models.

The atomic-level construction of Cz-COFs was further investigated by solid-state ¹³C cross-polarization magic-angle spinning (CP/MAS) NMR spectroscopy (Fig. S3, ESI[†]). The peaks at 157 ppm corresponding to the C atoms of the C=N linkages were observed for both COFs. Notably, the peaks at 148 ppm assigned to the carbon atoms bonding to the N atoms of the carbazole rings were also observed. The signals at 191 ppm for the end group of C=O almost disappeared, indicating that most aldehyde groups have been consumed in the condensation. Besides, another peak at 127 ppm was observed for Cz-COF2, which was assigned to the carbon atoms of the biphenyl edge units. Field emission scanning electron microscopy revealed that Cz-COFs have plate-like morphology (Fig. S4a and b, ESI[†]). High-resolution transmission electron microscopic images showed the presence of porous textures in Cz-COFs (Fig. S4c and d, ESI[†]).

Both Cz-COFs are highly crystalline polymers, as revealed by powder X-ray diffraction (PXRD) measurements. The

experimental PXRD pattern of Cz-COF1 displayed strong signals at 4.90° and 9.88° (Fig. 1a, red curve), which are assignable to the (110) and (220) facets, respectively. In addition, signals at 6.94°, 14.90°, and 22.32° corresponding to respectively the (200), (420), and (001) facets were also observed. Pawley refinement (Table S2, ESI[†]) using a C222 space group with lattice parameters of $a = 27.067$ Å, $b = 27.735$ Å, and $c = 3.993$ Å yielded a PXRD pattern (Fig. 1a, green curve) that agrees with the experimentally observed pattern, as indicated by their negligible difference (Fig. 1a, black curve). Similarly, Cz-COF2 exhibited strong signals at 3.99° (110) and 8.02° (220) together with peaks at 5.71° (200), 12.10° (420), and 21.78° (001) (Fig. 1b, red curve). Pawley refinement (Table S3, ESI[†]) using a C222 space group with lattice parameters of $a = 33.274$ Å, $b = 32.220$ Å, and $c = 3.976$ Å yielded a PXRD pattern (Fig. 1b, green curve) that can reproduce the experimental curve with small difference (Fig. 1b, black curve). These small differences were evidenced by their small R_{wp} (4.87%) and R_p (3.71%) values for Cz-COF1 and R_{wp} (3.61%) and R_p (2.83%) values for Cz-COF2, and suggest the correctness of the above PXRD assignments.

A density-functional tight-binding method, which included a Lennard-Jones dispersion, was used to simulate the optimum structures of Cz-COFs. From the calculations, there is only one possible orthorhombic crystal system for the COFs from the bicarbazole and diamines. Using the optimal monolayer structure, the AA and AB stacking models were generated and optimized. The bicarbazole molecule consists of two carbazole subunits connected with a N–N bond in which they are twisted owing to the steric hindrance of the protons on the proximate phenyl units. Indeed, their twisted angle is as high as 73.5° for the bicarbazole monomer. In the monolayer, the twisted angles decreased to 48.9° and 57.9° for Cz-COF1 and Cz-COF2, respectively, leading to more planar structures for the bicarbazole vertices. Notably, the twisted angles become much smaller in the stacked frameworks; the twisted angle is only 37.2° for Cz-COF1 and 42.1° for Cz-COF2. These decrements in the twist angle along with the formations of 2D polygon monolayer and frameworks are profound and indicate that the bicarbazole units although with an extremely large dihedral angle, can trigger a significant conformational change upon polycondensation and fit the two carbazole subunits into the 2D frameworks.

In the stacked structure, Cz-COF1 adopts an AA stacking model of a space group of C222 with $a = 27.3616$ Å, $b = 27.4776$ Å, and $c = 3.9778$ Å (Fig. 1a, upper inset, and Table S4, ESI[†]). The simulated PXRD pattern of the AA stacking model (Fig. 1a, blue curve) matched the experimental peak positions and intensities, whereas the staggered AB stacking model (Fig. 1a, yellow curve) did not reproduce the data. The staggered AB model (Table S5, ESI[†]) resulted in covered pores by the neighboring sheets (Fig. 1a, bottom inset). Similarly, Cz-COF2 also assumes an AA stacking model of a space group of C222 with $a = 33.1865$ Å, $b = 32.485$ Å, and $c = 3.9868$ Å (Fig. 1b, upper inset, and Table S6, ESI[†]). The simulated PXRD pattern of the AA stacking model (Fig. 1b, blue curve) also matched well the experimental peak positions and intensities, whereas the staggered AB stacking model (Fig. 1b, orange curve) did not

reproduce the data. The staggered AB model (Table S7, ESI[†]) significantly shelters the pores by the neighboring sheets (Fig. 1b, bottom inset).

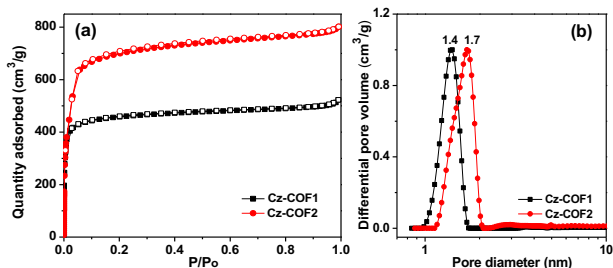


Fig. 2 (a) Nitrogen adsorption (filled symbols) and desorption (empty symbols) isotherms for the Cz-COFs collected at 77.3 K. (b) Pore size distribution curves calculated by using the NLDFT method.

Cz-COFs exhibited typical type I nitrogen gas sorption isotherms with a sharp nitrogen gas uptake at low relative pressure (Fig. 2a), featuring microporous materials.³¹ Cz-COF2 exhibited higher Brunauer-Emmet-Teller (BET) specific surface area ($2387 \text{ m}^2 \text{ g}^{-1}$, Fig. S9, ESI[†]) and pore volume ($1.24 \text{ cm}^3 \text{ g}^{-1}$) than Cz-COF1 ($1557 \text{ m}^2 \text{ g}^{-1}$ and $0.88 \text{ cm}^3 \text{ g}^{-1}$), which could be attributed to the longer biphenyl unit than the phenyl moiety at the edge parts, as also observed for other COFs.^{10,30} The theoretical accessible surface areas are 1889 and $2035 \text{ m}^2 \text{ g}^{-1}$ for Cz-COF1 and Cz-COF2, respectively (ESI[†]). Notably, the BET surface area of Cz-COF2 is much higher than those of most 2D COFs reported.^{32–35} Fig. 2b shows the pore size distribution curves calculated using nonlocal density functional theory (NLDFT). As predicated by the PXRD crystalline structures, Cz-COF1 and Cz-COF2 exhibited uniform pore size distribution with only one pore size of 1.4 and 1.7 nm, respectively. From the above structural characterizations, now it becomes clear that the bicarbazole COFs are crystalline porous materials with dense bicarbazole arrays and open 1D micropores (Scheme 1, bottom layer); these redox-active frameworks with open 1D porous structure enables the high accessibility of the redox-active sites to ions and electrons that are highly desired for energy storage.

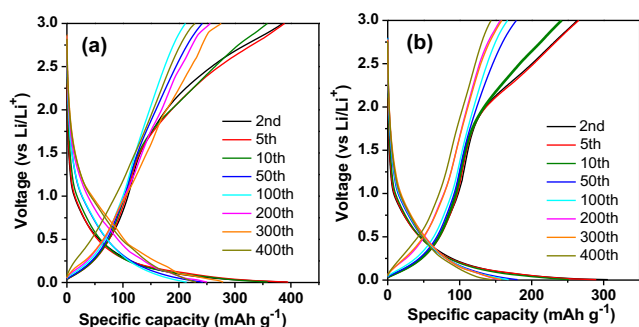


Fig. 3 Galvanostatic charge-discharge profiles of (a) Cz-COF1 and (b) Cz-COF2 at a current density of 200 mA g^{-1} .

The combination of dense redox-active bicarbazole arrays and ordered open micropores in one material makes Cz-COFs

ideal electrode materials for fabricating lithium ion batteries. We developed Cz-COFs as anode for CR2016 type coin cells assembled with Li counter electrode and 1.0 M LiPF₆ electrolyte (ESI[†]). The cyclic voltammetry (CV) profiles of both Cz-COFs showed a pair of asymmetric redox peaks in the potential region of 0–0.5 V (Fig. S10, ESI[†]), indicating the redox process of the Cz-COFs (Fig. S11, ESI[†]). Galvanostatic charge-discharge measurements were conducted in the potential range of 0.005–3 V (vs Li⁺/Li) at a current density of 200 mA g^{-1} . As shown in Figure 3, both Cz-COFs exhibited typical charge-discharge curves in the n-dopable potential region. The majority of capacity (> 80%) was achieved at a potential below 0.5 V, which suggests the facile doping of Li⁺ ions into the 1D channels of Cz-COFs.^{36,37}

The rate performance was investigated at different current densities up to 1000 mA g^{-1} (Fig. 4a). As a general tendency, Cz-COF1 shows higher capacity than Cz-COF2 at the same current density, as a result of the higher density of Cz units in the Cz-COF1 framework. Surprisingly, Cz-COF1 exhibited a capacity as high as 628 mAh g^{-1} at a current density of 100 mA g^{-1} . To the best of our knowledge, this capacity is much higher than those of the state-of-the-art porous organic polymers, such as PDCzBT (404 mAh g^{-1}),³⁸ BPPF (52 mAh g^{-1}),³⁹ and most other organic anode materials, such as HA (200 mAh g^{-1})⁴⁰ and Li₂BDP (200 mAh g^{-1}).⁴¹ We have synthesized an amorphous Cz-based porous polymer (Cz-CMP1) as control to show the advantages of using COFs (Figs. S12–S14, ESI[†]). Indeed, Cz-CMP1 shows much lower capacity of 313 mAh g^{-1} at a current density of 100 mA g^{-1} due to its low surface area and irregular pore size distribution (Fig. S15, ESI[†]). Intriguingly, both Cz-COFs exhibited high retention of the capacity at high current densities. Therefore, the ordered 1D pores facilitate ion transport and meet the requirement of rapid ion motion at high current density. These results indicate that the dense redox-active arrays and the ordered 1D pores work cooperatively in lithium redox reaction and lithium ion transport.

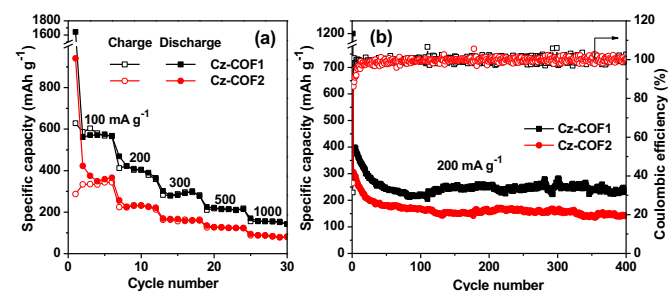


Fig. 4 (a) Rate performance of the Cz-COFs at varied current density ranging from 100 to 1000 mA g^{-1} . (b) Cycling performance and Coulombic efficiency of the Cz-COFs-based batteries.

We further investigated the cycle performance at a current density of 200 mA g^{-1} . Cz-COF1 and Cz-COF2 exhibited high retention of original capacities upon cycle and showed stable long-term performance. For example, after 400 cycles, Cz-COF1 exhibited a capacity as high as 236 mAh g^{-1} . Remarkably, the Coulombic efficiency is higher than 99% for both Cz-COFs (Fig. 4b), indicating that there is almost no energy loss during the

charge and discharge processes. These high performances rank the COFs a benchmark for energy storage with ultrahigh capacity, outstanding rate capability and long cycle life.

In summary, we have designed and synthesized novel bicarbazole-based COFs via the $[C_2 + C_2]$ topological diagram and Schiff-base condensation reaction. The Cz-COFs are highly crystalline, consist of dense arrays of redox-active bicarbazole sites, and possess high surface areas up to $2387 \text{ m}^2 \text{ g}^{-1}$. Owing to the synergistic effect of the dense redox-active arrays and the open 1D channels, the frameworks exhibited ultrahigh capacity, excellent rate capability and long cycle life. These profound results demonstrated the enormous potential of redox-active COFs as pre-designable electrode platform for the next-generation energy storage.

J.-X.J. thanks the National Natural Science Foundation of China (21574077 & 21304055), the Fundamental Research Funds for the Central Universities (GK201501002). D.J. thanks the Grant-in-Aid for Scientific Research (A) (17H01218) from MEXT, Japan for financial support.

Notes and references

- J. M. Tarascon, *Philos. Trans. R. Soc. A*, 2010, **368**, 3227.
- J. M. Tarascon, *Nat. Chem.*, 2010, **2**, 510.
- Y. Tang, Y. Zhang, W. Li, B. Ma and X. Chen, *Chem. Soc. Rev.*, 2015, **44**, 5926.
- F. Xu, X. Chen, Z. Tang, D. Wu, R. Fu and D. Jiang, *Chem. Commun.*, 2014, **50**, 4788.
- C. Zhang, X. Yang, W. Ren, Y. Wang, F. Su and J.-X. Jiang, *J. Power Sources*, 2016, **317**, 49.
- A. P. Cote, A. I. Benin, N. W. Ockwig, M. O'Keeffe, A. J. Matzger and O. M. Yaghi, *Science*, 2005, **310**, 1166.
- H. M. El-Kaderi, J. R. Hunt, J. L. Mendoza-Cortes, A. P. Côté, R. E. Taylor, M. O'Keeffe and O. M. Yaghi, *Science*, 2007, **316**, 268.
- X. Feng, X. S. Ding and D. Jiang, *Chem. Soc. Rev.*, 2012, **41**, 6010.
- S. Y. Ding and W. Wang, *Chem. Soc. Rev.*, 2013, **42**, 548.
- H. Furukawa and O. M. Yaghi, *J. Am. Chem. Soc.*, 2009, **131**, 8875.
- N. Huang, X. Chen, R. Krishna and D. Jiang, *Angew. Chem. Int. Ed.*, 2015, **54**, 2986.
- S. Dalapati, E. Jin, M. Addicoat, T. Heine and D. Jiang, *J. Am. Chem. Soc.*, 2016, **138**, 5797.
- G. Q. Lin, H. M. Ding, D. Q. Yuan, B. S. Wang and C. Wang, *J. Am. Chem. Soc.*, 2016, **138**, 3302.
- X. Feng, L. L. Liu, Y. Honsho, A. Saeki, S. Seki, S. Irlle, Y. P. Dong, A. Nagai and D. Jiang, *Angew. Chem. Int. Ed.*, 2012, **51**, 2618.
- L. Chen, K. Furukawa, J. Gao, A. Nagai, T. Nakamura, Y. P. Dong and D. Jiang, *J. Am. Chem. Soc.*, 2014, **136**, 9806.
- S. Chandra, T. Kundu, S. Kandambeth, R. BabaRao, Y. Marathe, S. M. Kunjir and R. Banerjee, *J. Am. Chem. Soc.*, 2014, **136**, 6570.
- H. Xu, S. Tao and D. Jiang, *Nat. Mater.*, 2016, **15**, 722.
- L. Stegbauer, K. Schwinghammer and B. V. Lotsch, *Chem. Sci.*, 2014, **5**, 2789.
- H. Xu, J. Gao and D. Jiang, *Nat. Chem.*, 2015, **7**, 905.
- Q. Sun, B. Aguila, J. Perman, N. Nguyen and S. Ma, *J. Am. Chem. Soc.*, 2016, **138**, 15790.
- Q. Sun, B. Aguila, J. Perman, L. D. Rarl, C. W. Abney, Y. Cheng, H. Wei, N. Nguyen, L. Wojtas and S. Ma, *J. Am. Chem. Soc.*, 2017, **139**, 2786.
- S. Y. Ding, M. Dong, Y. W. Wang, Y. T. Chen, H. Z. Wang, C. Y. Su and W. Wang, *J. Am. Chem. Soc.*, 2016, **138**, 3031.
- H. Yang, S. Zhang, L. Han, Z. Zhang, Z. Xue, J. Gao, Y. Li, C. Huang, Y. Yi, H. Liu and Y. Li, *ACS App. Mater. Int.*, 2016, **8**, 5366.
- F. Xu, S. B. Jin, H. Zhong, D. C. Wu, X. Q. Yang, X. Chen, H. Wei, R. W. Fu and D. Jiang, *Sci. Rep.*, 2015, **5**, 8225.
- H. Liao, H. Wang, H. Ding, X. Meng, H. Xu, B. Wang, X. Ai and C. Wang, *J. Mater. Chem. A*, 2016, **4**, 7416.
- L. Bai, Q. Gao and Y. Zhao, *J. Mater. Chem. A*, 2016, **4**, 14106.
- C. R. Deblase, K. Hernándezburgos, K. E. Silberstein, G. G. Rodríguezcalero, R. P. Bisbey, H. D. Abruña and W. R. Dichtel, *ACS Nano*, 2015, **9**, 3178.
- C. R. Mulzer, L. Shen, R. P. Bisbey, J. R. McKone, N. Zhang, H. D. Abruna and W. R. Dichtel, *ACS Cent. Sci.*, 2016, **2**, 667.
- Z. Zha, L. Xu, Z. Wang, X. Li, Q. Pan, P. Hu and S. Lei, *ACS Appl. Mater. Int.*, 2015, **7**, 17837.
- C. R. DeBlase, K. E. Silberstein, T. T. Truong, H. D. Abruna and W. R. Dichtel, *J. Am. Chem. Soc.*, 2013, **135**, 16821.
- K. S. W. Sing, D. H. Everett, R. A. W. Haul, L. Moscou, R. A. Pierotti, J. Rouquerol and T. Siemieniowska, *Pure Appl. Chem.*, 1985, **57**, 603.
- S. Y. Ding, J. Gao, Q. Wang, Y. Zhang, W. G. Song, C. Y. Su and W. Wang, *J. Am. Chem. Soc.*, 2011, **133**, 19816.
- R. Gomes, P. Bhanja and A. Bhaumik, *Chem. Commun.*, 2015, **51**, 10050.
- Y. L. Zhu, S. Wan, Y. H. Jin and W. Zhang, *J. Am. Chem. Soc.*, 2015, **137**, 13772.
- V. S. Vyas, F. Haase, L. Stegbauer, G. Savasci, F. Podjaski, C. Ochsenfeld and B. V. Lotsch, *Nat. Commun.*, 2015, **6**, 8508.
- L. Zhu, Y. Niu, Y. Cao, A. Lei, X. Ai and H. Yang, *Electrochim. Acta*, 2012, **78**, 27.
- K. Sakaushi, E. Hosono, G. Nickerl, T. Gemming, H. Zhou, S. Kaskel and J. Eckert, *Nat. Commun.*, 2013, **4**, 1485.
- S. Zhang, W. Huang, P. Hu, C. Huang, C. Shang, C. Zhang, R. Yang and G. Cui, *J. Mater. Chem. A*, 2015, **3**, 1896.
- K. Sakaushi, E. Hosono, G. Nickerl, H. Zhou, S. Kaskel and J. Eckert, *J. Power Sources*, 2014, **245**, 553.
- H. Zhu, J. Yin, X. Zhao, C. Wang and X. Yang, *Chem. Commun.*, 2015, **51**, 14708.
- S. Renault, V. A. Oltean, C. M. Araujo, A. Grigoriev, K. Edström and D. Brandell, *Chem. Mater.*, 2016, **28**, 1920.